

Article

Research on the Correlations between Spatial Morphological Indices and Carbon Emission during the Operational Stage of Built Environments for Old Communities in Cold Regions

Fei Zheng *, Yuqing Wang, Zhicheng Shen and Yuetao Wang

College of Architecture and Urban Planning, Shandong Jianzhu University, Jinan 250101, China

* Correspondence: 12914@sdjzu.edu.cn

Abstract: The escalation of the urban population and energy demands has exacerbated the carbon emission intensity at the operational stage of urban old communities. The spatial elements of the built environments comprising building groups, roads and landscape, and the spatial morphology of these elements, are endowed not only with human activities but also impact local microclimates and overall carbon emissions. Nonetheless, little attention has been paid to the correlation mechanism between the spatial morphology of the urban built environments and carbon emissions. In this paper, the aim is to combine carbon emissions simulation and statistical analysis to find the correlation between the spatial morphological indices and carbon emissions and to bridge the gaps. Thus, guided by the principles of urban energy modeling, this research adopts a parametric process of “information model construction–carbon emission simulation–statistical analysis”. First, taking 60 typical samples of an old community in Jinan, China, as objects, morphological indices such as density, texture and layout are analyzed through regression analysis to highlight their impacts on carbon emissions. Then, a carbon emission prediction model based on spatial morphological indices is established and verified. The results show that the floor area ratio (FAR), building coverage ratio (BCR), enclosure degree (ED), shape factor (SF) and average road aspect ratio (AS) have significant impacts on carbon emissions during the operational stage. Among these indices, the FAR and the ED are identified as the pivotal influencers. The findings confirm the important role of spatial morphological design of old communities in cold regions in improving urban carbon reduction potential, and they provide theoretical underpinnings and empirical data as references for urban morphology design formulated within the context of low-carbon objectives.

Keywords: urban morphology; carbon emission; old communities; regression analysis; cold region



Citation: Zheng, F.; Wang, Y.; Shen, Z.; Wang, Y. Research on the Correlations between Spatial Morphological Indices and Carbon Emission during the Operational Stage of Built Environments for Old Communities in Cold Regions.

Buildings **2023**, *13*, 2222. <https://doi.org/10.3390/buildings13092222>

Academic Editor: Peng Du

Received: 29 June 2023

Revised: 25 August 2023

Accepted: 28 August 2023

Published: 31 August 2023



Copyright: © 2023 by the authors. Licensee MDPI, Basel, Switzerland. This article is an open access article distributed under the terms and conditions of the Creative Commons Attribution (CC BY) license (<https://creativecommons.org/licenses/by/4.0/>).

1. Introduction

Climate change is an issue of common concern to the global society. Extreme climate events caused by excessive carbon emissions have seriously affected the human living environment. The 2015 Paris Climate Conference not only adopted the first fair global agreement to deal with global warming, but it also aimed to limit the increase in temperature to 2 °C before 2100 [1]. In recent years, international standard-writing organizations have published the latest UNI EN ISO 14064:2018 and UNI EN ISO 14064:2019 [2–4] (Parts 1, 2 and 3) to improve the comparability and science of carbon footprint calculations across countries [5].

Human activity in cities is a major source of CO₂ emissions and a contribution to climate change [6]. As an important component of urban residential land, old communities have received much attention due to the influence of their spatial morphology on building energy consumption [7]. Traditional urban planning tends to adopt a large-scale building unit and high-density building layout [8]. This planning mode took less into account the impact of the spatial morphological indices of urban residential land on building energy consumption and carbon emissions [9]. In fact, urban planning and spatial optimization

are playing an important role in the mitigation of CO₂ emissions at an urban level [10]. Traditionally, studies assessing the environmental impact of urban morphology had focused on GHG emissions caused by the operational stage of (a) buildings [11] (b), urban transport [12] (c) or both [13,14].

Carbon emission in cities is composed of the carbon source and carbon sink from activities of various land use properties [15]. Carbon source land shows different carbon emission characteristics through different land use properties. Carbon sink land shows different degrees of carbon clearing and carbon absorption capacity according to different land use properties. According to the data of the International Energy Agency, urbanized areas consume 60% of the world's energy and produce more than 70% of the world's carbon emissions [16,17]. The building industry accounts for one-third of global energy consumption, accounting for 28% of CO₂ emissions, of which residential buildings account for the largest proportion of energy consumption [18]. The carbon emission of urban residential land is an important part of urban carbon emission. In 2020, the carbon emissions of urban residential building in China during the operational phase totaled 901 million tons, accounting for 42% of the national building carbon emissions [19]. Studies evaluating the impact of urban spatial morphological indices on carbon emissions mainly focused on the operational stage [20]. Cuéllar-France and Azapagic used the LCA method to evaluate the carbon emissions of three common residential buildings in the UK, which were divided into three stages: the construction stage, operational stage and waste disposal stage. It was found that the carbon emissions in the operational stage contributed the most [21]. Based on the LCA method, Huang et al. calculated the carbon emissions in the whole life cycle of residential buildings in Shanghai and pointed out that the two stages of building materials' production and operation have the largest carbon emissions [22]. In addition, studies have also found that carbon emissions in the operational stage account for 70–90% of the whole life cycle carbon emissions [23–25]. Thus, it can be seen that the key to the peak of building carbon emissions is to control the carbon emissions in the construction operational stage. As the basic unit of energy consumption and carbon emissions in urban residential buildings, old communities produce a large amount of detectable data in their long life cycle, which has important practical conditions for carbon reduction research in the operational stage.

Meanwhile, research shows that there is a close correlation between carbon emissions, energy consumption and energy utilization in old communities, and the correlation is even more pronounced in cold areas [26,27]. A study by Chen Jialiang analyzed the relationship between the energy consumption and morphology of the northern community in the background and found that the distance from the sea, the construction time and the building height are the three most important factors affecting the residential energy consumption [28]. Comparing the energy consumption of Chinese and foreign buildings, Jiang Yi concluded that building energy consumption mainly depends on the difference in energy consumption mode and climate environment [29]. Professor Zhang Jie discovered in his research that in the cold region, where Jinan is located, the highest energy consumption method is electricity, followed by heating energy consumption [30]. Therefore, it is natural for people to believe that achieving energy-saving and emission reduction goals for residential buildings in cold regions will face even greater challenges.

Furthermore, the energy consumption of residential buildings is also affected by the local microclimate [31]. The formation of local microclimate is closely related to the urban spatial form [32]. Therefore, the spatial morphology of the built environment for old communities affects the balance of the internal microclimate, including air temperature, relative humidity, wind speed, wind direction and other microclimate elements, which then affects the energy consumption of heating and cooling and ultimately affects carbon emission during the operational stage. Through the simulation of the physical environment of residential communities with different spatial morphology, Xuan Wei investigated how incorporating a reasonable spatial design can enhance the microclimate environment of residential communities and effectively lower energy consumption and carbon emissions [33].

In addition, the utilization of solar energy has gradually become an important issue for the construction industry to implement the carbon reduction path [34]. On the one hand, the acquisition of sunlight will reduce lighting energy consumption. On the other hand, solar radiant heat reduces heating and cooling energy consumption by increasing solar energy production capacity, which reduces carbon emissions from non-renewable energy use. A large number of studies have verified that the morphological indices of residential buildings have a great influence on the acquisition of solar radiation [35–38]. Tathiane, Adolphe et al. studied the influence of different morphological indices on solar energy utilization potential. The results show that increasing the aspect ratio of the block is more conducive to increasing the acquisition of solar radiation than increasing the floor area ratio [39]. A study by Kruger et al. found that the north–south orientation of the building group can produce shading effects between buildings and reduce carbon emissions from building HVAC systems [40]. It can be seen that the improvement of the morphology of old communities can have a positive effect on energy saving and carbon reduction, whether from the perspective of the influence mechanism of space itself on the comfort of living environment or spatial planning on the implementation of auxiliary technology paths.

As shown above, although the influence of spatial morphology on building performance and energy consumption has been discussed, most of the studies focused on the single aspect of buildings and the urban level. There are few studies on the correlation between the spatial morphological indices of the old communities and carbon emissions, especially in cold regions. Studies are usually targeted at severe cold regions or mild climate zones. If considering only the single building morphology, it is easy to ignore the influence of the layout of the building group on the heat dissipation and heat demand of the building [41,42]. Additionally, the height, shape, shape factor, length of continuous building interface and size of the public area of the internal buildings in old communities may have an impact on the level of building energy consumption [43,44]. Accordingly, in the present study, we focused on the impact of spatial morphological indices of old communities on carbon emissions in cold regions. By quantitatively analyzing its underlying mechanisms, the study reveals the carbon reduction potential of building clusters in spatial planning and renovation within cities. Specifically, this is theoretically significant in guiding the urban building energy conservation and carbon reduction policies from the perspective of urban planning.

Given this background, the aim of this work is to quantitatively analyze the influence mechanism of spatial morphological indices of old communities on carbon emission and determine which factors play the greatest role in carbon reduction in order to provide recommendations to carry out low-carbon-oriented urban planning in the future.

In the cold region city of Jinan, China, 60 typical old communities are selected as research objects. This research starts by emphasizing the influence mechanism of urban morphology on carbon emission and expounding the knowledge gaps in the research and literature on carbon emissions in old communities. The Section 2 selects the study samples and explains the methodological approach. In Section 3, the results of this study are presented through three subsections: simulation of carbon emissions in old communities, calculation of morphological indices and statistical analysis of correlation between variables. The Section 4, further discusses how the spatial morphological indices of the old community affect carbon emission and the perspective of spatial morphological planning strategies towards carbon reduction. The Section 5 summarizes the conclusion of this paper, which is that the design of spatial morphology for old communities in cold regions has a significant impact on reducing carbon emissions during their operational stage.

2. Study Area and Methods

2.1. Study Area

The cold regions of China mainly refer to areas where the average temperature of the coldest month is $-10-0$ °C, and the daily average temperature of 5 °C is present for 90~145 days. Jinan is one of the representative cities in the cold region. According to

the “2023 urban old community renovation plan table” and “Jinan 2023 old community renovation task table” issued by Jinan City, the article selected the old communities in the central urban area of Jinan City as the research object, which can represent the overall basic morphology of old communities and guide planning and renovation design. The distribution points of the sample area of the old community are shown in Figure 1a. The FAR and BCR of the sample area are significantly reduced from the center to the periphery (Figure 1b,c).

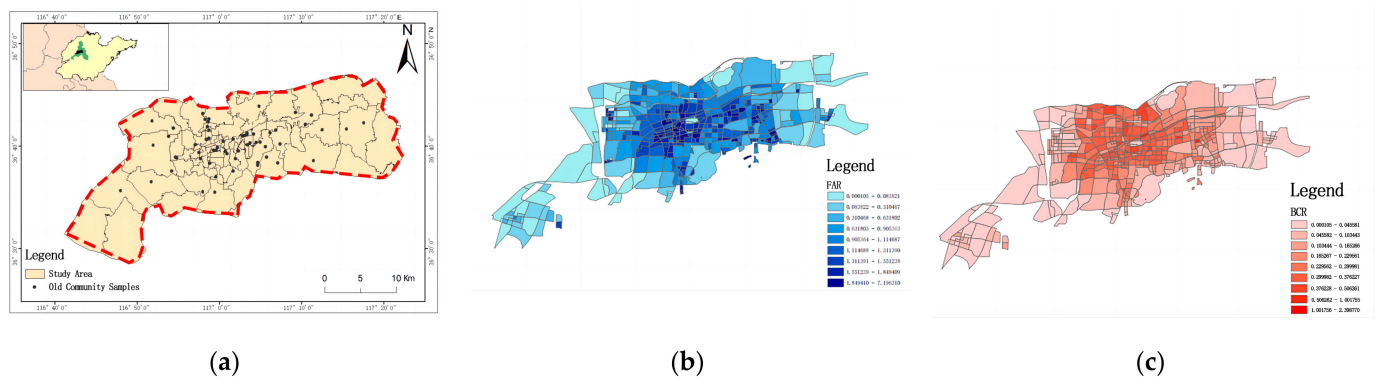


Figure 1. (a) Distribution of old community samples; (b) Distribution of FAR in the study area; (c) Distribution of BCR in the study area.

2.2. Methods

Currently, the research methods for building carbon emission and energy consumption are relatively mature. With the emphasis on urban energy consumption and carbon emissions, researchers began to expand the concept of building energy conservation and emission reduction design to the field of urban design. Accordingly, the urban energy modeling method (urban building energy modeling, UBEM) emerged. Swan and Ugursal divided the modelling approach into top-down and bottom-up approaches [39–45]. The gray box method as one of the bottom-up methods is used in this study. The gray box method can predict energy demand and energy consumption in urban areas by combining the physical model method and the data analysis method and integrating them into a model [46–51]. Since this model can perform statistical analysis of three types of data, including climate parameters, building geometry and non-geometric information, considering local microclimate and urban morphology, it can be applied to the simulation of energy consumption and carbon emission of old communities in cold regions.

Based on the UBEM method, this research constructs a parametric analysis process of “information model construction–carbon emission simulation–statistical analysis” to study the influence mechanism of spatial morphological indices and carbon emission of old communities.

The process is divided into four modules (Figure 2): (1) Parameter preset module: Use ArchGis10.6.1 software to identify the spatial morphological indices of the old community and obtain the building type, envelope structure, energy load and other parameters of the old community samples combined with the research content; (2) Shape generation module: Based on the identification of morphological indices, UMI-Site [52], Grasshopper and other plug-ins are used to calculate the morphological indices and the construction of the old community model; (3) Performance calculation module: The UWG operator is used to simulate the microclimate of the old residential area. The results are presented in the EPW meteorological data file. Then, the EPW file is imported into UMI for carbon emission simulation; (4) Data analysis module: Based on the statistical analysis method, the calculation value of the spatial morphological indices and the carbon emission simulation value are analyzed accordingly.

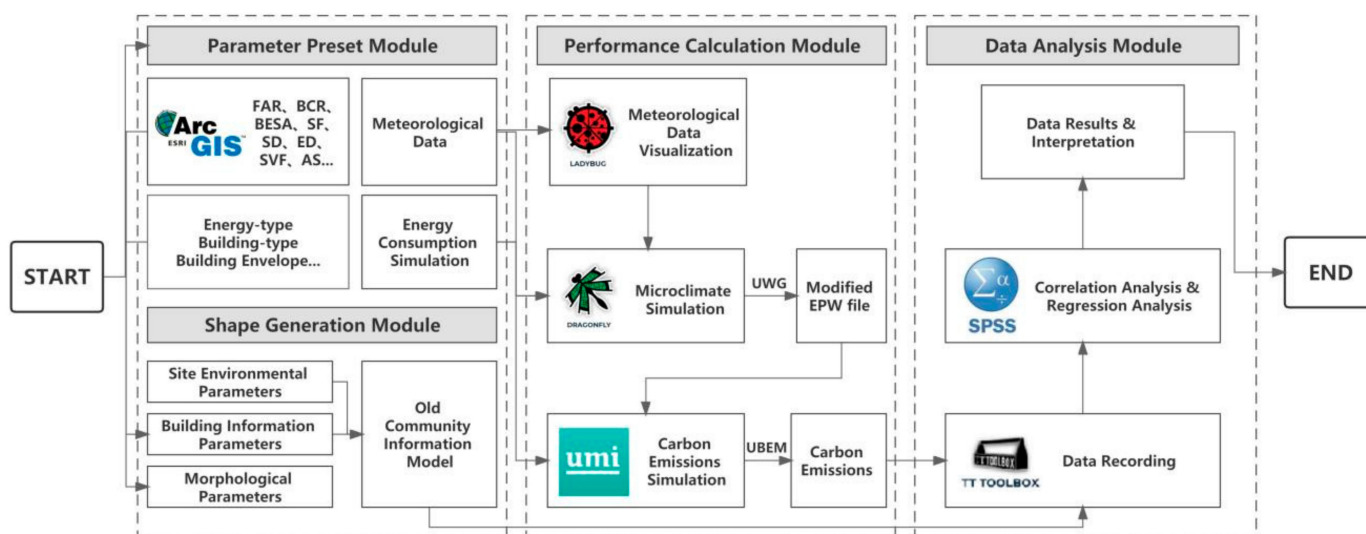


Figure 2. Process of “information model construction–carbon emission simulation–statistical analysis”.

2.2.1. The Construction of Building Information Model

The building information model includes the following parts: climate data, building geometric data and non-geometric data of buildings.

- Acquisition of climate parameters

The climate parameters of Jinan City were extracted through the ladybug. The average temperature in Jinan is 14.7 °C, and the coldest month is January, with an average temperature of −0.4 °C. The hottest month is July, with an average temperature of 27.5 °C. The dominant wind direction is southwest and northeast, followed by east, north and south. Northwest wind is the least dominant. The summer and winter climate characteristics in Jinan are different: the summer temperature is hot, with an average temperature of 26.7 °C. This season is not only hot but also rainy, with the characteristics of hot rain in the same season. The average air temperature in the winter is about 1 °C.

- Construction of the geometric model of the old community

At first, geometric data, such as the outline and morphology of old plots, are captured by Google satellite map. Then, we use the Grasshopper1.0.0007 platform to filter and identify 3D data (shp data) of buildings and sites, extracted and classified according to the gis data in the satellite openstreetmap. The 3D information model of the old community was established in Rhino to facilitate editing in the energy consumption simulation platform. Next, we use the @it plug-in to identify and extract the shp file, establish the geometric information of the site and building and use the excel plugin to extract the dbf file containing the building height and layer information, giving the height information to the building block, and finally generate the geometry model of old communities.

- Input of building non-geometric attribute information

Building non-geometric attribute information can be provided by the plug-in Template Library Editor, which is a standalone application in UMI for creating, managing and editing XML Template Library Files (TLF). TLF files can exchange and store information regarding the materials, structures, schedules, heat loads and morphology. By editing the template of building parameters in the TLF file, non-geometric information of old residential areas for carbon emission simulation can be obtained (Figure 3).

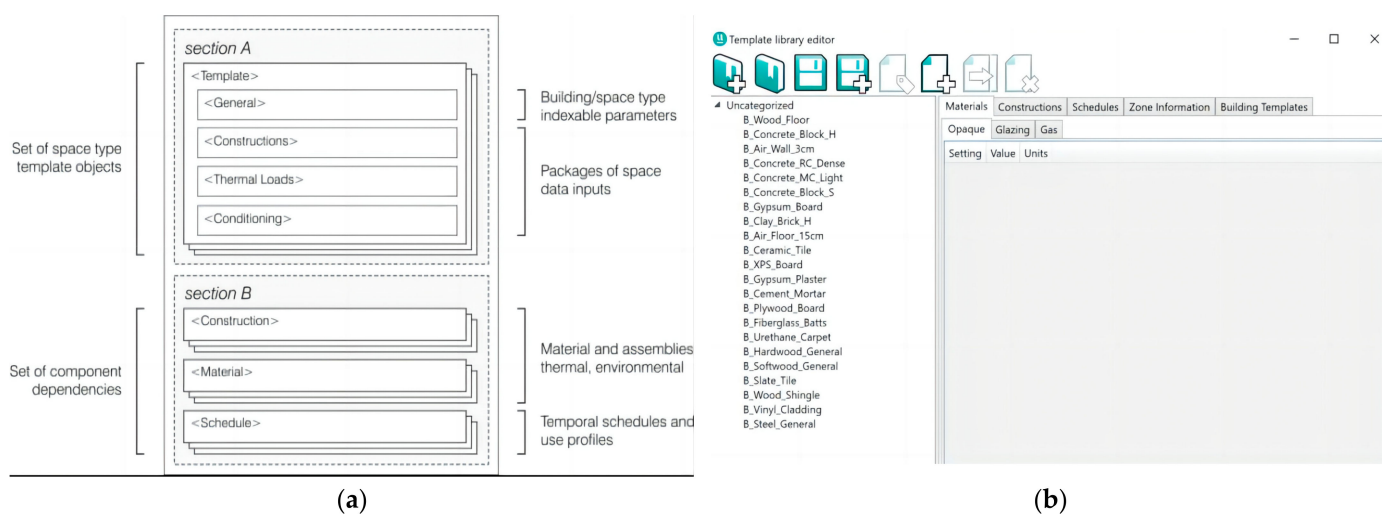


Figure 3. (a) Establish TLF template; (b) UMI-TLF extractor.

2.2.2. Extraction and Measurement of Morphological Indices

- Extraction of the morphological indices

Prof. Meta Berghauser Pont, University of Delft, The Netherlands, proposed a chart to evaluate the association between morphological density and urban morphology. She combined the four morphological density indices of building floor area ratio, building density, average number of floors and open space rate. She named them as “Spacemate” [53], which can reflect the possibility of climate resources entering inside the complex. Urban morphological texture can reflect the organizational structure between material entities and space in the urban environment, and it has an important impact on the construction of local microclimate within the building complex [54]. Considering the comprehensive description of the space morphology of the old area and the influence of climate resources in the area, this research selected the floor area ratio (FAR) and building coverage ratio (BCR) as the morphological density indices. Additionally, we selected building exterior surface area (BESA), shape factor (SF), enclosure degree (ED), scattered degree (SD), aspect ratio (AS), sky visual factor (SVF) as morphological texture indices. The above eight indices can comprehensively describe and evaluate the overall spatial morphology quality of the old community [55]. In addition, the old community can be divided into four categories—point-type, slab-type, mixed-type and enclosed-type—based on its architectural form.

- Calculation of morphological indices

The advantages of parametric modeling lie in its ability to describe the geometric features of building morphology in the form of data information [56]. FAR and BCR can be directly measured in the site module of the UMI. Gross floor area (m^2) can calculate the total building area. Site ground area can calculate the area of the site. Floor area ratio can calculate the building floor area ratio. Occupants can calculate the bottom area of the building. Thus, BCR can be obtained. BESA, SF, ED, SD, AS need to be obtained from the three-dimensional information of the building and site model. The following table (Table 1) summarizes the connotation and extraction methods of different morphological indices. The extraction results of sample morphology are shown in Table 2.

Table 1. Morphological indices.

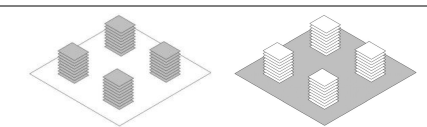
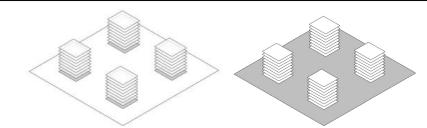
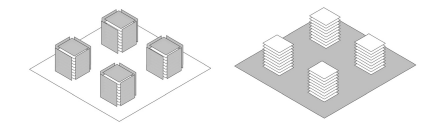
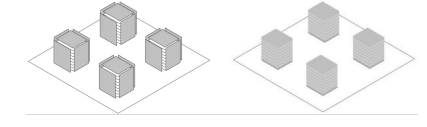
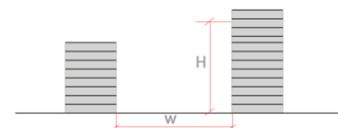
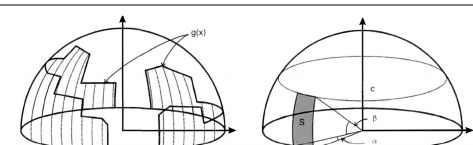
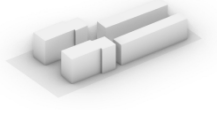
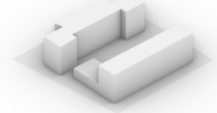
Morphological Indices	Formula	Connotation	Extraction Method	Schematic Diagram
Floor Area Ration (FAR)	FAR = Gross Floor Area/Site Area Reflects the spatial distribution characteristics of buildings	FAR = Gross Floor Area/Site Area Reflects the spatial distribution characteristics of buildings	UMI-Site Module	
Building Coverage Ratio (BCR)	BCR = Floor Space/Site Area	Reflects the density of urban or regional buildings		
Building Exterior Surface Area (BESA)	BESA = Building Exterior Surface Area/Site Area	Reflects the ability of the outer surface of the building to absorb solar radiation		
Shape Factor (SF)	SF = Building Exterior Surface Area/Volume	Reflects the complexity of the building form and the surface area of the enclosure structure	Grasshopper Module	
Enclosure Degree (ED)	ED = Building Façade Length/Building Control-Line Length	Reflects the openness and closure of a region or space		-
Scattered Degree (SD)	SD = Height Max-Height Average	Reflects the degree of dispersion of buildings in an area or space		-
Average Road Aspect Ratio (AS)	AS = Height Average /Road Width	Reflects the basic morphological unit formed by buildings and roads on both sides of the road in the plot		
Sky View Factor (SVF)	-	Reflects the shielding degree of building density, height and shape from the surrounding environment	ShadingMask Module	

Table 2. Sample morphology.

Type	Samples				
Slab-type					...
Point-type					...
Mixed-type					...
Enclosed-type					...

2.2.3. Carbon Emission Simulation

- Simulation parameter setting

This research uses the physical model method and the performance calculation module to calculate the carbon emission intensity of the old community.

Based on the sample research and literature review, this research uses the control variable method to characterize the control of building thermal parameters. Parameters related to physical simulation, such as building plane form and window to wall ratio, are excluded to exclude the interference of building monomer from the simulation results. According to the provisions of heat transfer coefficient and thermal inertia in the “Design Standard for Energy Efficiency of Residential Buildings in Severe Cold and Cold Areas (JGJ26-2018)” [57], combined with the investigation results of thermal parameters of old residential areas, this research obtained the main envelope structure parameters of old residential areas for carbon emission simulation (Table 3).

Table 3. Thermal parameters of building envelope.

Enclosure Structure	Exterior Wall	Floor Slab	Window	Roof	Partition Wall
Heat Transfer Coefficient (W/(m ² ·K))	1.6	1.5	3.0 (SHGC = 0.6; South/North Window–Wall Ratio = 0.35; East/West Window–Wall Ratio = 0)	1.0	1.0

Secondly, it is necessary to set the energy consumption parameters of the sample area. In the energy consumption simulation, the “schedule” refers to the operational mode of various equipment, lighting, heating, ventilation and other systems in the building in different time periods. The “schedule” can accurately calculate the energy consumption and carbon emissions by simulating the daily use of the equipment. The “schedule” is usually composed of a series of time periods and values in the building simulation software. Each period corresponds to a time range, such as a specific period of the day, and the value of the period represents the running state of the system during that period. This

research combines the “Code for Design of Heating Ventilation and Air Conditioning of Civil Buildings (GB50736-2012)” [58], “Green Performance Calculation Standard for Civil Buildings (JGJT449-2018)” [59] and the energy consumption survey results of the sample area to set the energy consumption parameters of the construction equipment during the operational stage (Table 4).

Table 4. Energy consumption parameter setting.

Parameter Type		Parameter Settings		
HVAC System	Type	Domestic Split Air Conditioner		
		Natural Gas Heating		
	Energy Efficiency	Refrigeration Energy Efficiency Ratio	2.3	
		Heating Energy Efficiency Ratio	1.9	
	Temperature	Refrigeration	7:00 am–8:00 pm, 20 °C 8:00 pm–7:00 am, 18 °C	
		Heating	7:00 am–8:00 pm, 26 °C 8:00 pm–7:00 am, 27 °C	
Occupants	Density	0.025 per/m ²		
	Indoor Activity	7:00 pm–8:00 am, 1 h 8:00 am–9:00 am and 6:00 pm–7:00 pm, 0.7 h 9:00 am–6:00 pm, 0.3 h		
Domestic Water	Time Period	7:00 am–12:am and 9:00 pm–11:00 pm, 1 h 12:00 am–1:00 pm, 0.6 h 6:00 pm–9:00 pm, 0.2 h		
Lighting System	Illuminance	200 lux		
	Lighting Power Density	7 W/m ²		
	Illuminating Period	7:00 am–8:00 am and 10:00 am–12:00 am and 11:00 pm–12:00 pm, 0.2 h 8:00 am–10:00 am and 7:00 pm–8:00 pm, 0.5 h 8:00 pm–12:00 pm, 0.8 h		
Equipment System	Power	5 W/m ²		
	Time Period	1:00 am–6:00 am, 0.2 h 7:00 am–8:00 am and 6:00 pm and 11:00 pm–12:00 pm, 0.6 h 9:00 pm–11:00 pm, 0.8 h 7:00 pm–9:00 pm, 1 h		

- Simulation result

First, the microclimate conditions need to be the output parameters. The research simulates the microclimate according to the following three steps: building morphology setting, urban morphology setting and simulation operation. Second, the microclimate EPW file of the sample old village will be imported into UMI-Energy to measure the carbon emission. The carbon emission simulation of the UMI plug-in is part of its full life cycle (LC) module. Currently, this module only allows the calculation of the basic implicit environmental impact related to building materials and does not apply to the calculation of the impact of carbon emissions during the operation stage. Hence, carbon emissions in the operational phase must be converted by obtaining energy consumption results in the operational energy module. This module can obtain the annual total energy consumption and energy consumption per unit area of lighting, heating, refrigeration, equipment, domestic water and gas in the sample area (Figure 4). Based on the IPCC method, the simulation results of various energy sources are multiplied by their carbon emission factors (Table 5) to obtain the carbon emissions per unit area of each energy source. Finally, the carbon emissions of various types are summarized to obtain the overall carbon emissions per unit area, namely the carbon emission intensity.

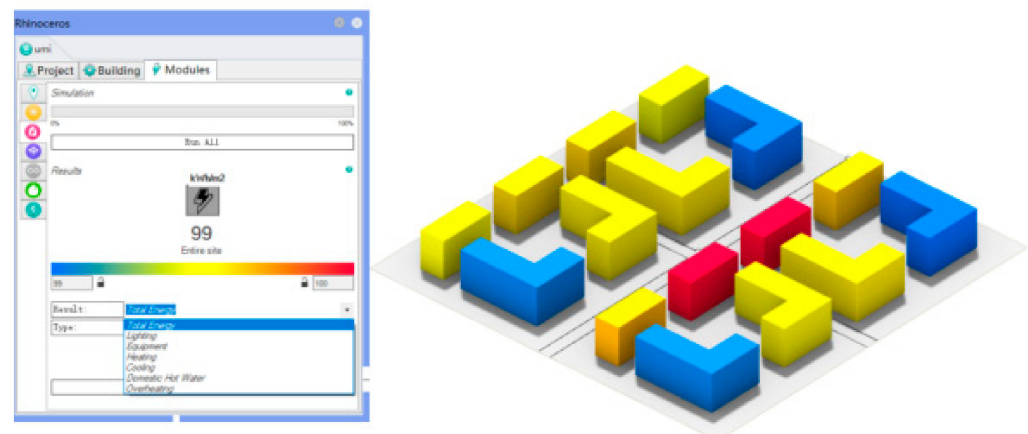


Figure 4. Operating energy computing module.

Table 5. Carbon emission factors.

	Energy Consumption Unit	Factor	Source	Carbon Emission Units
Electrical Energy	kWh/month	0.758	Ministry of Science and Technology of China	KgCO ₂ /kWh
Combustion Gas	m ³ /month	0.232	Ministry of Science and Technology of China	KgCO ₂ /kWh
Domestic Water	t/month	2.77	The China Energy Management Network	KgCO ₂ /m ³

2.2.4. Statistical Analyses

This section uses correlation analysis and multiple linear regression analysis of the statistical analysis method to establish a carbon emission prediction analysis model based on the spatial morphological indices of old communities in order to establish the influence mechanism of different morphological indices and carbon emissions.

- Correlation analysis

This research uses the Pearson correlation analysis to test whether there is a correlation between independent variables and dependent variables and to establish a correlation matrix to screen morphological indices, eliminating parameters with strong collinearity. At the same time, correlation analysis can explain the influence of single variables on different types of old communities. Pearson correlation analysis explains the strength and direction of the relationship between the two variables. The Pearson correlation coefficient is usually represented by r , with values ranging from -1 to 1 , where 0 indicates no linear correlation, 1 represents a complete positive correlation, and -1 represents a complete negative correlation.

- Multiple linear regression analysis

Using the morphological indices as independent variables, the prediction analysis model of carbon emission was established to predict the overall carbon emission values of samples. Finally, the actual data are selected to test the error of the regression equation to ensure its scientific nature. The regression equation can more specifically show the key morphological indices and their influence laws, which affect the carbon emissions of old communities.

3. Results

3.1. Spatial Morphological Indices

After the establishment of 60 sample models, this section calculates and counts the morphological indices of the old residential areas and draws the box plot of morphological distribution. The statistical morphological parameter information is shown in the following table (Table 6). Categories A, B, C and D refer to slab-type, point-type, mixed-type and enclosed-type, respectively. According to the calculation results and the distribution

map of different morphological indices (Figure 5), it can be found that the BESA of the enclosed-type buildings is high, and the SD of point-type buildings is large, with a high body complexity. According to the morphological calculation data, the ED of the enclosed-type building group is the largest; meanwhile, the SD of the mixed-type building group is the largest. In addition, the SVF of the slab-type building group is the largest, indicating that there is a good vision and mutual occlusion level in slab-type old communities. Furthermore, the enclosed-type buildings have the highest FAR and BCR, which indicates that the enclosed-type building group has high land development intensity, while the land development intensity of the other old communities is insufficient. Moreover, the AS of the point-type building group is at a high level, followed by mixed-type buildings.

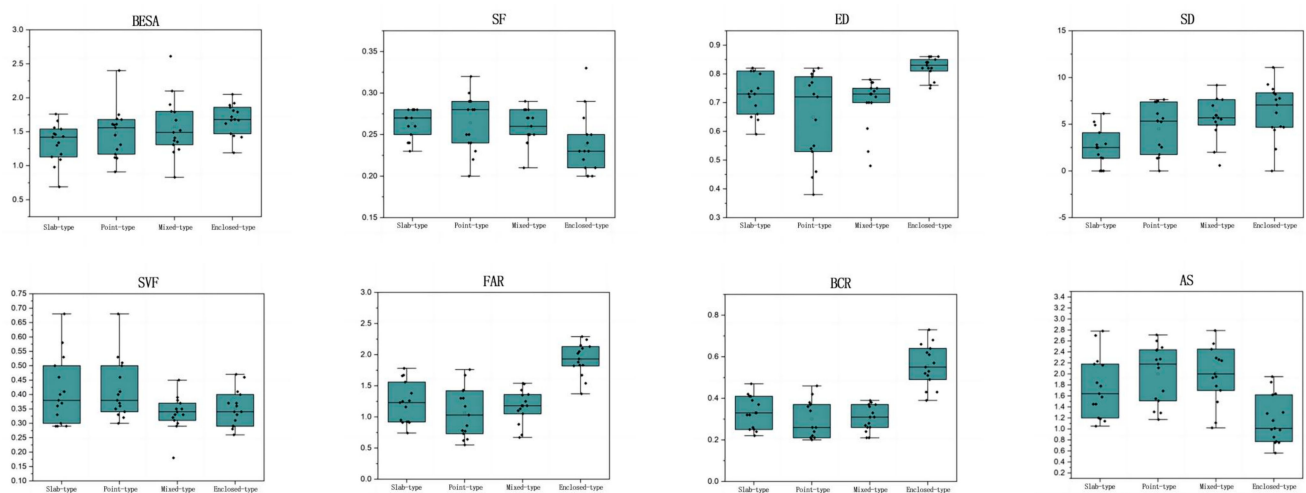


Figure 5. Data distribution of morphological indices for sample old communities.

Table 6. Statistical results of morphological indices.

	BESA	SF	ED	SD	SVF	FAR	BCR	AS
A-1	0.98	0.26	0.74	2.50	0.29	1.25	0.32	1.45
A-2	1.30	0.25	0.81	4.10	0.40	1.36	0.39	1.2
A-3	1.46	0.24	0.8	2.50	0.38	1.67	0.41	1.84
A-4	1.43	0.28	0.82	2.90	0.29	1.07	0.37	1.14
A-5	1.42	0.27	0.72	4.90	0.29	1.42	0.42	1.43
A-6	0.69	0.28	0.7	0	0.58	1.01	0.22	1.88
A-7	1.66	0.27	0.73	0	0.30	1.16	0.26	1.64
A-8	1.47	0.24	0.81	2.50	0.33	1.56	0.41	1.15
A-9	1.34	0.28	0.69	1.4	0.37	0.92	0.25	1.18
A-10	1.54	0.26	0.67	0	0.41	1.21	0.24	1.82
A-11	1.56	0.28	0.81	2.8	0.36	0.91	0.25	1.05
A-12	1.13	0.27	0.73	5.25	0.5	1.23	0.32	1.45
A-13	1.09	0.28	0.79	1.36	0.53	0.92	0.33	1.58
A-14	1.17	0.26	0.75	6.13	0.68	1.26	0.33	1.71
A-15	1.76	0.23	0.82	0	0.46	1.08	0.47	1.62
B-1	1.61	0.29	0.45	1.40	0.37	0.70	0.20	2.18
B-2	1.24	0.29	0.55	0	0.41	0.77	0.22	1.51
B-3	1.11	0.24	0.81	2.80	0.36	1.21	0.42	1.49
B-4	1.75	0.28	0.64	5.25	0.50	0.96	0.24	2.13
B-5	1.12	0.24	0.8	1.36	0.53	1.32	0.37	2.26
B-6	0.91	0.25	0.77	6.13	0.68	1.3	0.34	1.05
B-7	1.69	0.32	0.73	1.75	0.46	1.17	0.26	1.17
B-8	2.40	0.22	0.46	2.53	0.51	0.84	0.21	2.27
B-9	1.68	0.23	0.68	7.63	0.34	1.21	0.46	1.69
B-10	1.56	0.29	0.52	5.32	0.3	0.62	0.21	2.44

Table 6. Cont.

	BESA	SF	ED	SD	SVF	FAR	BCR	AS
B-11	1.61	0.25	0.76	7.4	0.35	0.91	0.36	1.31
B-12	1.45	0.20	0.79	5.36	0.4	0.98	0.37	2.43
B-13	1.6	0.28	0.58	7.39	0.38	0.78	0.38	1.55
B-14	1.31	0.28	0.72	5.62	0.32	1.03	0.26	1.14
B-15	1.17	0.30	0.53	7.53	0.33	0.73	0.21	1.24
C-1	1.31	0.24	0.78	5.25	0.35	1.43	0.37	1.28
C-2	0.83	0.28	0.7	4.90	0.38	1.05	0.26	1.36
C-3	1.35	0.26	0.74	0.58	0.37	1.25	0.33	2.26
C-4	2.61	0.28	0.61	7.00	0.18	1.46	0.24	1.02
C-5	1.49	0.27	0.73	4.38	0.35	1.18	0.28	2.79
C-6	1.90	0.21	0.7	19.04	0.32	1.1	0.27	2.45
C-7	2.10	0.28	0.7	2.00	0.33	1.13	0.26	2.55
C-8	1.37	0.25	0.75	5.95	0.34	1.35	0.36	1.11
C-9	1.8	0.29	0.53	5.67	0.31	0.77	0.21	1.93
C-10	1.79	0.27	0.73	9.17	0.39	1.18	0.31	1.95
C-11	1.67	0.25	0.77	5.68	0.45	1.53	0.38	1.49
C-12	1.2	0.24	0.76	5.94	0.29	0.92	0.21	2.79
C-13	1.52	0.25	0.75	7.63	0.33	1.36	0.37	2.24
C-14	1.24	0.27	0.72	5.53	0.35	1.18	0.31	1.7
C-15	1.41	0.25	0.77	7.71	0.3	1.54	0.39	1.78
D-1	1.19	0.24	0.81	2.33	0.37	1.67	0.73	0.75
D-2	1.86	0.27	0.83	4.67	0.29	1.88	0.55	0.99
D-3	1.89	0.22	0.88	0.00	0.28	2.02	0.52	1.85
D-4	2.05	0.33	0.91	4.38	0.31	2.15	0.51	0.85
D-5	1.92	0.20	0.86	6.22	0.33	1.89	0.49	1.64
D-6	1.47	0.23	0.84	8.75	0.29	1.93	0.43	1.95
D-7	1.42	0.21	0.86	4.67	0.46	1.82	0.43	1.3
D-8	1.67	0.29	0.84	11.08	0.26	1.54	0.39	1.62
D-9	1.81	0.25	0.75	8.2	0.47	1.37	0.53	1.01
D-10	1.79	0.25	0.96	7.77	0.4	2.05	0.68	0.62
D-11	1.62	0.23	0.82	9.25	0.37	2.13	0.66	0.76
D-12	1.68	0.23	0.82	7.06	0.41	2.29	0.64	0.77
D-13	1.72	0.21	0.88	8.36	0.34	2.1	0.62	0.54
D-14	1.44	0.20	1	7.63	0.36	1.83	0.61	0.56
D-15	1.67	0.20	0.95	4.74	0.34	2.24	0.57	0.62

3.2. Results of the Carbon Emission Simulation

In this section, the annual energy consumption of various types of energy in the sample old communities is simulated through the energy module of the UMI plug-in. Then, the energy consumption is converted into carbon emissions per unit area through the carbon emission factors (Table 7).

Table 7. Simulation results of carbon emissions per unit area during the operational stage.

Carbon Emissions (KgCO ₂ /m ²)		Carbon Emissions (KgCO ₂ /m ²)		Carbon Emissions (KgCO ₂ /m ²)		Carbon Emissions (KgCO ₂ /m ²)	
A-1	74.28	B-1	86.41	C-1	72.77	D-1	63.67
A-2	72.01	B-2	78.83	C-2	75.80	D-2	68.22
A-3	70.49	B-3	70.49	C-3	74.28	D-3	68.98
A-4	72.77	B-4	78.07	C-4	78.07	D-4	69.74
A-5	75.80	B-5	72.77	C-5	75.04	D-5	69.74
A-6	78.83	B-6	73.53	C-6	75.80	D-6	69.74
A-7	75.04	B-7	75.04	C-7	75.80	D-7	70.49
A-8	71.25	B-8	81.11	C-8	73.53	D-8	72.77
A-9	76.55	B-9	70.49	C-9	80.35	D-9	73.53
A-10	78.07	B-10	84.14	C-10	75.04	D-10	65.95
A-11	77.32	B-11	73.53	C-11	72.77	D-11	65.95
A-12	75.04	B-12	72.77	C-12	80.35	D-12	65.95
A-13	76.56	B-13	78.83	C-13	73.53	D-13	65.95
A-14	74.28	B-14	75.80	C-14	75.04	D-14	66.70
A-15	69.74	B-15	79.59	C-15	72.77	D-15	67.46

According to the box plot of carbon emissions per unit area for old communities (Figure 6), it can be observed that the overall distribution of carbon emissions per unit area of the slab-type building group is relatively uniform, with a median value of approximately $74 \text{ KgCO}_2/\text{m}^2$, which suggests that there is not much variation in carbon emissions between the slab-type buildings in the sample. Additionally, the box plot shows that the median carbon emissions per unit area for point-type buildings are relatively high, at approximately $76 \text{ KgCO}_2/\text{m}^2$, indicating that there are more individuals with high carbon emissions for the point-type building group. Furthermore, the median carbon emissions per unit area for mixed-type neighborhoods are approximately $75 \text{ KgCO}_2/\text{m}^2$, similar to slab-type and point-type buildings, and the distribution of carbon emissions is also relatively uniform. Notably, the overall carbon emissions per unit area for enclosed-type old neighborhoods are relatively low, with a relatively concentrated distribution and a median value of approximately $67 \text{ KgCO}_2/\text{m}^2$.

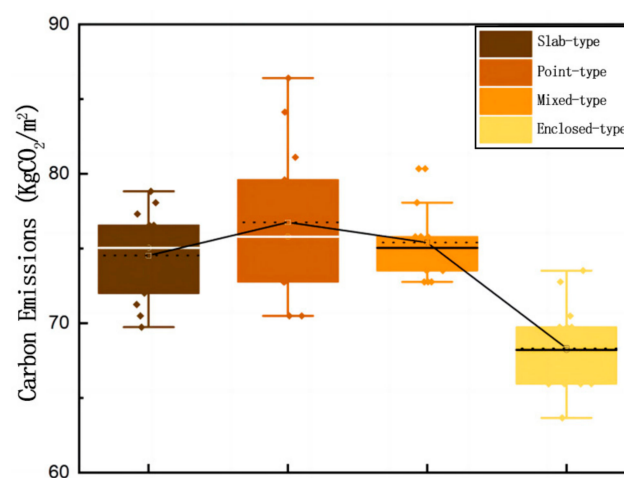


Figure 6. Box plots of carbon emission distribution of four types of old communities.

3.3. Statistical Analysis

3.3.1. Correlations between Morphological Indices and Carbon Emission

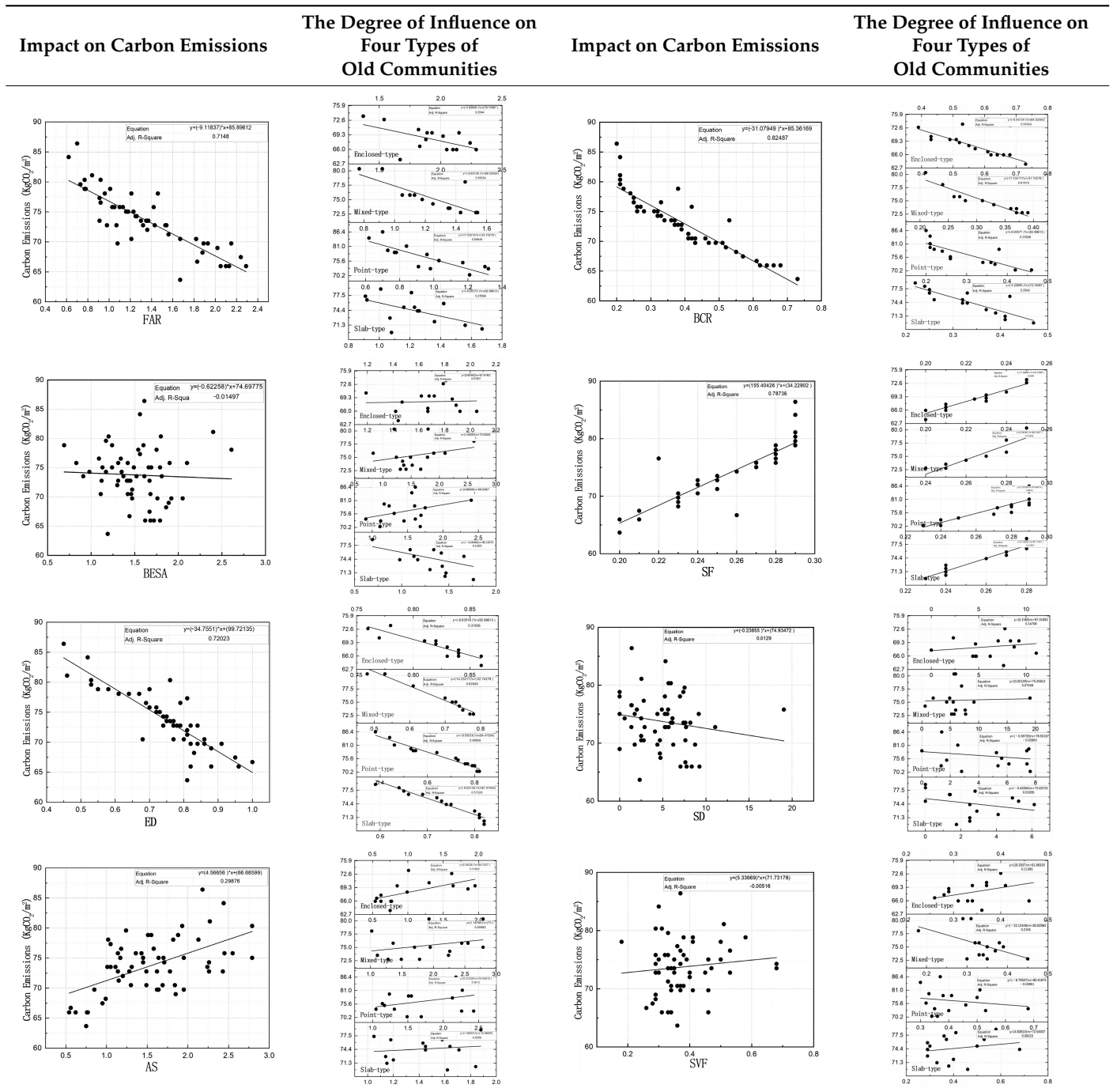
The calculated results of the eight spatial morphological indices obtained with correlation analysis are shown in Table 8.

- FAR

According to the research sample data, the overall FAR is in the range of 0.70–2.24, which is slightly lower than the standard level. The scatter plot shows that there is a significant correlation between carbon emissions and FAR. The carbon emissions per unit area for samples with FAR between 1.5 and 2.5 exhibit a relatively large degree of dispersion. The R^2 and partial regression coefficient (B) values of the fitted equation are 0.758 and -7.07 , respectively. This suggests that there is a certain negative linear correlation between the carbon emission intensity per unit area and the FAR for samples within the range of 0.35 to 2.77 in terms of FAR. On the whole, with the increase in FAR, the overall building aggregation degree in the old community increases, resulting in the reduction in heat island effect and heat dissipation, which reduces the heating energy consumption in the community, thus affecting the overall carbon emission level of the old community.

Furthermore, from the quadratic regression results, there is a strong negative linear correlation between the point-type and the mixed-type building group and the carbon emissions per unit area. On the whole, the influence degree of floor area ratio on the four building types is ranked as follows: point-type > mixed-type > slab-type > enclosed-type.

Table 8. Correlation analysis of morphological indices and carbon emission.



- BCR

There is a clear linear fitting relationship between BCR and carbon emissions. The R2 and partial regression coefficient (B) values of the fitted equation are 0.824 and -31.107949 , showing a high linear negative correlation. Based on the quadratic regression results of BCR and carbon emissions for the four building types, the influence degree of BCR on carbon emissions is ranked as follows: point-type > mixed-type > slab-type > enclosed-type.

- BESA

The results show that there is a linear trend between carbon emission intensity and BESA, but the R2 of the two fitting equations is only 0.015, indicating that the linear

relationship between the two is not significant enough, and the data are more scattered. From the quadratic regression analysis results, there are differences in the relationship between the BESA and the carbon emission intensity. The BESA fits the carbon emission intensity in different cell types. This means that the BESA may not be a major factor affecting the carbon intensity.

- SF

The SF refers to the relationship between the shape of the building and the aerodynamic performance of the building, and it is also an important index used to measure the heat transfer ability of the buildings. The R2 and partial regression coefficient (B) values of the fitted equation are 0.78736 and 155.40428, which indicates that there is a significant positive correlation between the SF and the carbon emission intensity. From the quadratic regression results, it can be found that the influence degree of SF on the carbon emissions of four building types is ranked as follows: point-type > slab-type > mixed-type > enclosed-type.

- ED

The results show that the R2 and partial regression coefficient (B) values of the fitted equation are 0.72 and -34.755 , indicating that there is a significant negative correlation between them. The larger the ED, the lower the heat loss of the building. This means that increasing the ED to a certain degree can reduce the heating energy consumption of buildings, thereby lowering the overall carbon emissions of the old communities. From the quadratic regression results, it can be found that the influence degree of SF on the carbon emissions of four building types is ranked as follows: point-type > slab-type > mixed-type > enclosed-type.

- SD

The R2 of the fitting equation of carbon emission per unit area and SD in old communities is 0.0129, and the partial regression coefficient (B) is -0.23955 , indicating that there is no obvious linear correlation between the two. From the perspective of the quadratic regression result, the patchwork of the four types of buildings does not show an obvious linear trend of carbon emission per unit area and a large dispersion degree, which means that the SD is not the main factor affecting the overall carbon emission per unit area of the old communities.

- AS

The scatter plot between the AS and the carbon emission intensity shows a certain linear trend. However, the R2 and partial regression coefficient (B) values of the fitted equation are 0.299 and 4.56656, indicating that there is a certain degree of positive correlation between the AS and carbon emissions. In general, with the increase in the AS, the carbon emission intensity of old communities increases.

- SVF

The results show that the R2 of the linear fitting equation between the SVF and the carbon emission intensity is 0.005, while the partial regression coefficient (B) is 5.33669, which means that there is a certain positive correlation between the carbon emission intensity and the SVF.

3.3.2. Regression Analysis of the Morphological Indices and Carbon Emission

- Establishing the correlation indices

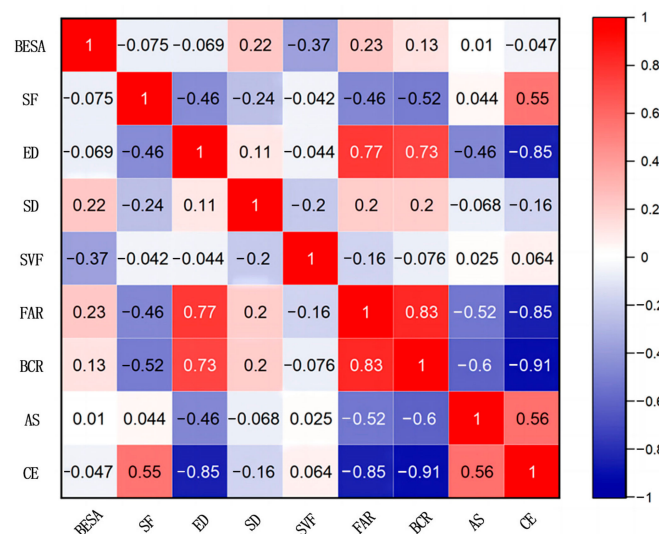
After identifying the linear relationship between morphological indices and unit carbon emissions per unit area during the operational stage, the research establishes a Pearson correlation coefficient matrix based on morphological indices and unit carbon emissions per unit area. Finally, highly correlated non-collinear morphological indices are selected for multiple linear regression analysis (Table 9).

Table 9. Correlation matrix between morphological indices and carbon emissions.

		BESA	SF	ED	SD	SVF	FAR	BCR	AS	Carbon Emission
BESA	Correlation Coefficient	1	−0.075	−0.052	0.232	−0.371 **	0.231	0.13	0.01	−0.047
	Significance		0.571	0.69	0.074	0.004	0.076	0.322	0.94	0.72
	Numbers	60	60	60	60	60	60	60	60	60
SF	Correlation Coefficient	−0.075	1	−0.453 **	−0.254	−0.042	−0.461 **	−0.517 **	0.044	0.547 **
	Significance	0.571		0	0.05	0.751	0	0	0.74	0
	Numbers	60	60	60	60	60	60	60	60	60
ED	Correlation Coefficient	−0.052	−0.453 **	1	0.128	−0.057	0.772 **	0.736 **	−0.477 **	−0.851 **
	Significance	0.69	0		0.329	0.664	0	0	0	0
	Numbers	60	60	60	60	60	60	60	60	60
SD	Correlation Coefficient	0.232	−0.254	0.128	1	−0.197	0.201	0.212	−0.068	−0.172
	Significance	0.074	0.05	0.329		0.132	0.123	0.104	0.608	0.188
	Numbers	60	60	60	60	60	60	60	60	60
SVF	Correlation Coefficient	−0.371 **	−0.042	−0.057	−0.197	1	−0.16	−0.076	0.025	0.064
	Significance	0.004	0.751	0.664	0.132		0.221	0.565	0.852	0.629
	Numbers	60	60	60	60	60	60	60	60	60
FAR	Correlation Coefficient	0.231	−0.461 **	0.772 **	0.201	−0.16	1	0.830 **	−0.525 **	−0.848 **
	Significance	0.076	0	0	0.123	0.221		0	0	0
	Numbers	60	60	60	60	60	60	60	60	60
BCR	Correlation Coefficient	0.13	−0.517 **	0.736 **	0.212	−0.076	0.830 **	1	−0.600 **	−0.910 **
	Significance	0.322	0	0	0.104	0.565	0		0	0
	Numbers	60	60	60	60	60	60	60	60	60
AS	Correlation Coefficient	0.01	0.044	−0.477 **	−0.068	0.025	−0.525 **	−0.600 **	1	0.563 **
	Significance	0.94	0.74	0	0.608	0.852	0	0		0
	Numbers	60	60	60	60	60	60	60	60	60
Carbon Emission	Correlation Coefficient	−0.047	0.547 **	−0.851 **	−0.172	0.064	−0.848 **	−0.910 **	0.563 **	1
	Significance	0.72	0	0	0.188	0.629	0	0	0	
	Numbers	60	60	60	60	60	60	60	60	60

** At the 0.01 level, the correlation was significant.

As shown in the figure below (Figure 7), there is no significant correlation observed between SD, SVF and the unit area carbon emissions of old communities. The remaining indices have some correlation with carbon emissions, which can be used as independent variables for regression analysis. To avoid the collinearity problem of the morphological indices, the BCR with strong collinearity is removed. Finally, multiple linear regression analysis is conducted on the four independent variables, namely AS, FAR, ED and SF.

**Figure 7.** Heat map of correlation between morphological indices and carbon emission.

- Multiple linear regression analysis

In this section, a Pearson multiple linear regression equation including AS, FAR, ED and SF is established to predict the carbon emissions per unit area of old communities. According to Table 10, the R² of the model is 0.855, which indicates that the change in the independent variable could explain 85.5% of the variance of the dependent variable. The adjusted R² value of 0.923 reflects the model's fitting effect, which takes into account the number of independent variables used in the model.

Table 10. The fitting degree of model.

Model	R	R ²	Adjusted R ²	Standard Error of Estimate	Durbin–Watson
1	0.925	0.855	0.845	1.813167	1.971

The regression coefficient table provides an indication of the degree to which each independent variable affects the dependent variable (Table 11). The absolute values of the standardized coefficients for FAR and ED are relatively larger, at 0.241 and 0.628, respectively, indicating that they have a greater impact on unit area carbon emissions. By contrast, the absolute values of standardized coefficients for AS and SF are relatively smaller, at 0.149 and 0.111, respectively, indicating that they have a smaller impact on unit area carbon emissions (Figure 8).

Table 11. The regression result of morphological indices.

Model	Partial Regression Coefficient		Standardized Regression Coefficient	t	Statistical Significance	Collinearity		
	B	Standard Error	Beta			Tolerance	VIF	
(constant)	81.927	4.21		19.458	0			
1	FAR	− 3.731	0.936	− 0.347	− 3.987	0	0.348	2.877
	SF	28.76	9.527	0.186	3.019	0.004	0.696	1.437
	ED	− 17.078	3.358	− 0.42	− 5.086	0	0.386	2.59
	AS	1.44	0.513	0.178	2.808	0.007	0.655	1.527

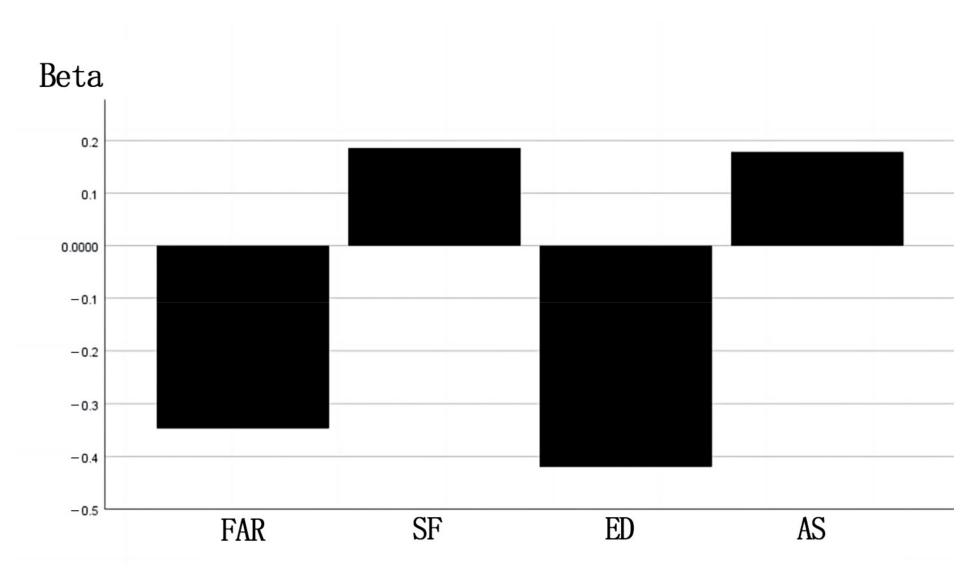


Figure 8. Comparison of standardization coefficients.

Furthermore, the regression coefficients of FAR, SF, ED and AS in this model are -3.731 , 28.76 , -17.078 and 1.44 , respectively. Thus, the regression equation is

$$y = -3.731 * \text{FAR} + 28.76 * \text{SF} - 17.078 * \text{ED} + 1.44 * \text{AS} + 81.927 \quad (1)$$

After the regression equation was determined, the sample data of 15 old communities in Tianjin [60], which belong to cold regions, were selected to verify the validity of the regression equation, including 3 point-type, 7 slab-type and 5 enclosed-type building groups (Table 12). The results indicate that the average error between the measured value and predicted value is 1.09%, suggesting that the prediction model is reasonably accurate (Figure 9). In other words, the regression results can provide a useful reference for studying the relationship between the spatial morphological indices and carbon emission at the operational stage of old communities in cold regions.

Table 12. The comparison of measured carbon emissions and predicted carbon emissions.

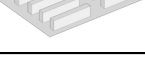
No.	Layout Type	FAR	SF	ED	AS	Measured Value of Carbon Emission (KgCO ₂ /m ²)	Prediction of Carbon Emission (KgCO ₂ /m ²)
A01	 Slab-type	1.91	0.26	0.74	1.45	78.58	80.95
A02	 Enclosed-type	1.33	0.25	0.81	1.20	75.56	77.33
A03	 Enclosed-type	1.51	0.24	0.82	1.84	74.49	78.05
A04	 Slab-type	1.38	0.28	0.80	1.14	71.77	78.15
A05	 Slab-type	1.29	0.27	0.72	2.18	79.80	80.96
A06	 Slab-type	1.30	0.25	0.77	2.71	76.43	79.96
A07	 Slab-type	1.87	0.27	0.73	1.64	80.04	81.50
A08	 Enclosed-type	1.36	0.24	0.81	2.70	71.25	78.91
A09	 Point-type	1.75	0.28	0.69	1.18	76.64	81.88
A10	 Enclosed-type	1.58	0.20	0.86	1.54	73.14	76.18
A11	 Slab-type	1.67	0.24	0.81	2.11	79.39	78.99

Table 12. Cont.

No.	Layout Type	FAR	SF	ED	AS	Measured Value of Carbon Emission (KgCO ₂ /m ²)	Prediction of Carbon Emission (KgCO ₂ /m ²)
A12	 Point-type	1.23	0.27	0.73	1.45	75.04	79.74
A13	 Point-type	1.09	0.28	0.66	1.58	76.56	81.50
A14	 Slab-type	1.65	0.26	0.75	2.78	78.48	81.56
A15	 Enclosed-type	1.78	0.23	0.82	2.23	77.74	78.97

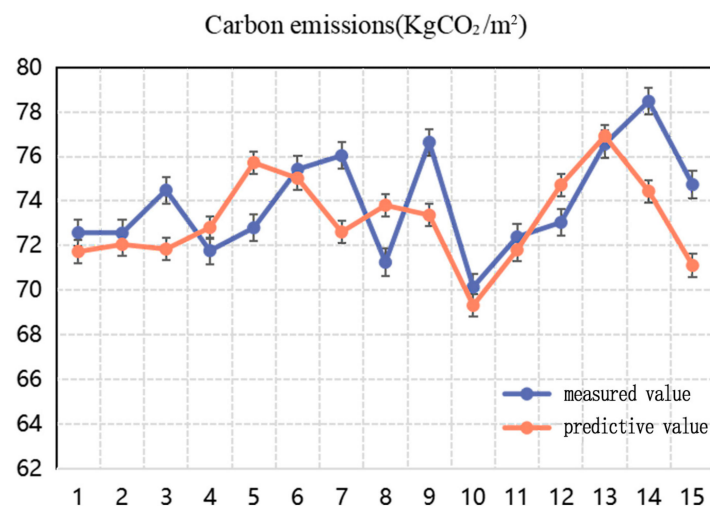


Figure 9. Comparison of measured carbon emissions and predicted carbon emissions.

4. Discussion

4.1. Result Analysis

4.1.1. Impact of Morphological Density Indices on Carbon Emission

Morphological density indices are important bases to measure the capacity of the residential area. Observing the sample distribution of old communities, it can be found that different FAR values will bring diversified spatial morphology characteristics. An increase in FAR will lead to an increase in building volume, which has an impact on ventilation and lighting. For the old communities with low development intensity, appropriately increasing the FAR of the old communities can contribute to the natural ventilation effect inside the organization, which is conducive to the reduction in energy consumption and carbon emission. The results also show that appropriately increasing the FAR of the old communities can reduce the carbon emission per unit area of the whole community, and the impact degree increases sharply after rising to 1.25. Among them, the FAR has the greatest impact on the carbon emission of the mixed-type building group and the least impact on the enclosed-type building group. Therefore, it is suggested to set the FAR above 1.25 for old communities. In the face of the current situation of low density in the old communities, in the low-carbon renewal of the old communities, we can consider extending the façade function of the old communities and appropriately increasing the basic function facilities and other operations to increase the FAR. BCR also has an important impact on ventilation

and lighting. High building density will lead to a smaller distance between the buildings, and the crowded space will have a negative impact on ventilation and natural lighting, aggravating the energy consumption and carbon emissions of the buildings themselves.

4.1.2. Impact of Morphological Texture Indices on Carbon Emissions

The morphological texture indices are the reflection of the three-dimensional spatial state of the old community. From the perspective of energy flux, the spatial morphological indices of the community play a great role in the simulation of carbon emission for the community.

The statistical results confirm that the AS is closely related to the carbon emissions of the old community. High buildings will affect the surrounding wind speed and ventilation, resulting in heat accumulation and poor circulation, so as to increase the energy consumption of air conditioning and carbon emission intensity of old communities. If the AS of the built environment is large, the height of the building is relatively low, which usually means that the air circulation is not smooth. It means that buildings require more energy consumption to maintain a comfortable indoor temperature. to maintain a comfortable indoor temperature. Based on the results of this research, the AS is positively correlated with the carbon emission of old communities.

According to the results, the SF has an obvious negative correlation with the carbon emission per unit area of the old communities. The smaller the SF of the building, the smaller the surface area of the building, the lower the heat transfer efficiency, and the lower the energy consumption. On the contrary, the larger the SF of the building, the greater the surface area of the building, the higher the heat transmission efficiency, and the higher the energy consumption, which affects the overall carbon emission of the old community. Therefore, in the process of low-carbon renewal of the old community, it is appropriate to reduce the complexity of residential buildings as far as possible and to select a more regular volume to reconstruct the space of the old community. The design of the building should minimize the SF to reduce energy consumption and improve energy efficiency.

In addition, the research shows that there is a correlation between ED and carbon emissions of the old community. On the one hand, the suitable open space layout can adjust the microclimate environment of old communities and reduce the carbon emission intensity of buildings. On the other hand, it can open the spacing between the buildings and avoid aggravating the shielding effect between them.

4.1.3. Impact of Morphological Layout Type on Carbon Emissions

Morphological layout types have a significant impact on carbon emissions from old residential areas in cold regions. From the perspective of the building types proposed in this paper, the carbon emission of enclosed-type buildings is lower than that of other types of old communities. The fundamental reason is that the high heating demand in cold regions is large, and the high enclosure degree can avoid the heat loss in residential areas in the winter. Therefore, it is suggested that the degree of buildings should be increased as much as possible in the design of old communities in cold regions.

4.2. Perspectives

Urban morphology has gradually become an important factor, which architects pay attention to in studying urban low-carbon renewal [61]. Nowadays, scholars are not only limited to research of the low-carbon renewal strategy of the building monomer, but they also pay much more attention to the influence of different regions or types of urban morphology on building energy consumption and carbon emission. In this research, we verified the close connection between the spatial morphological indices of the built environment of old communities and carbon emission in the operational stage, and we also emphasized that urban morphology can be used as an effective way of saving building energy and reducing carbon emission in cities in cold regions. Thus, urban planners and policy makers can help better understand the carbon emissions of old communities,

formulate more effective emission reduction measures and ultimately achieve the goal of sustainable urban development.

On the other hand, with the development of big data and artificial intelligence, digital technology has had an enormous impact on the field of architectural design and urban planning. The enhanced computing power enables UBEM technology to integrate more performance simulation technologies and apply them in the urban design field [62]. For example, Leng Hong et al. proposed the application of “auxiliary energy-saving-oriented urban design” as the application of urban morphology research results [63], that is, to assist the formulation of building energy-saving-oriented urban design scheme by studying the influence of urban morphology on building energy consumption and carbon emission. In this regard, this research established a statistical prediction model of carbon emission based on spatial morphological indices to evaluate the influence of spatial morphology on carbon emission at different mesoscales and finally obtained morphological indices and influence laws with significant effects. Based on this, the study provides guidance for low-carbon-oriented urban morphology renewal strategies by quantitatively analyzing the relationship between eight specific spatial morphological indices and carbon emissions: in cold regions, residential area renewal can increase the compactness of neighborhood buildings while ensuring basic functional requirements are met, increasing block enclosure and reconfiguring building façades to reduce the shape factor. Additionally, this research model can incorporate the construction status and morphological characteristics of different old cities to expand the types of spatial morphological indices, thus providing more targeted guidance for the formulation of control indices related to spatial morphology in low-carbon-oriented new urban planning.

Furthermore, there are still some limitations to be solved and discussed. Due to the difficulty in obtaining the data of carbon emissions in a large range of old communities, the representative small sample size of this paper is selected, and the regression model is verified by converting the energy consumption data into carbon emissions. In addition, based on the influence mechanism of urban morphology on carbon emission from the perspective of spatial design, this research selects eight morphological indices to form the spatial morphology parameter system of old communities. While these indices possess a degree of typicality, they nonetheless remain insufficiently comprehensive. Moreover, with respect to environmental factors, such as the greening rate of the site, underlying surface materials, as well as human factors, such as users’ energy consumption habits, this research adopted relative standard values in the model instead of conducting an in-depth exploration at this level. Nevertheless, the method of this research still provides a new possibility to study the relationship between spatial morphological indices and carbon emission of old communities with limited sample statistics and data acquisition conditions.

5. Conclusions

This research quantitatively examines the correlation between spatial morphological indices and carbon emission during the operational stage of built environments for old communities in cold regions. Specifically, 60 samples of old residential areas located in Jinan, a cold area, were selected for analysis. By combining numerical simulation and statistical analysis, this research conducted a comprehensive examination of the eight spatial morphological indices comprising three types of indices characterizing the morphological density, morphological texture and morphological layout of old communities. The final results show that

1. Of the four types of building groups outlined in this research, namely point-type, slab-type, mixed-type and enclosed-type, it was found that the total carbon emissions of the point-type and mixed-type building groups were relatively high, while the carbon emissions of the slab-type building group fell in the middle. Conversely, the carbon emissions per unit area of the enclosed-type building group were relatively low;
2. Among the morphological density and texture indices, the FAR, BCR and ED have obvious negative correlation with the carbon emission of old communities, while the

SF and AS are positively correlated with the carbon emission of old communities and have different degrees of influence on different layout types of old communities. Specifically, FAR and ED play a pivotal role in shaping point-type communities, although their influence on enclosed-type communities is minimal. BCR and SF have the greatest influence on point-type communities and the least influence on enclosed-type communities. In addition, AS only has an obvious impact on old communities with an enclosed layout. The other morphological indices have a weak impact on the carbon emissions of the old communities;

3. A multiple linear regression analysis was performed to develop a statistical predictive model of carbon emissions in old communities. The fitted equation yielded an R2 value of 0.855, signifying that the variations in independent variables, such as FAR, SF, ED and AS, can account for up to 85.5% of the variance in carbon emissions per unit area of the dependent variable;
4. FAR and ED are the primary indices, which significantly impact carbon emissions in old communities, with ED demonstrating the most pronounced effect. Keeping all other indices constant, each unit increase in FAR results in a 3.7% reduction in the carbon emission per unit area, while a unit increase in ED leads to an even greater reduction of 17.1%;
5. In essence, enhancing the spatial morphology of built environments in cold regions is a crucial factor in bolstering the carbon reduction potential of older communities in these areas.

Author Contributions: Conceptualization, F.Z. and Y.W. (Yuqing Wang); methodology, Y.W. (Yuqing Wang); software, Z.S.; validation, F.Z. and Y.W. (Yuetao Wang); formal analysis, Y.W. (Yuetao Wang); investigation, Z.S.; resources, Z.S.; data curation, F.Z. and Y.W. (Yuqing Wang); writing—original draft preparation, Y.W. (Yuqing Wang) and Z.S.; writing—review and editing, Y.W. (Yuqing Wang); visualization, F.Z.; supervision, Y.W. (Yuetao Wang); project administration, F.Z.; funding acquisition, F.Z. All authors have read and agreed to the published version of the manuscript.

Funding: This research received no external funding.

Data Availability Statement: Data available on request due to restrictions, e.g., privacy or ethics.

Acknowledgments: The authors are grateful for the support from the College of Architecture and Urban Planning at Shandong Jianzhu University. In addition, the authors would like to thank all the students of the Forward Architecture Study Society for their support in this research.

Conflicts of Interest: The authors declare no conflict of interest.

References

1. Laurent Fabius, Opening Speech by Laurent Fabius—Paris Climate Conference. 2015. Available online: <http://www.diplomatiegouv.fr/en/french-foreign-policy/climate/events/> (accessed on 2 May 2023).
2. *ISO 14064-1:2018; Greenhouse Gases-Part 1: Specification with Guidance at the Organization Level for Quantification and Reporting of Greenhouse Gas Emissions and Removals*. ES-UNE: Madrid, Spain, 2018.
3. *ISO 14064-2:2019; Greenhouse Gases—Part 2: Specification with Guidance at the Project Level for Quantification, Monitoring and Reporting of Greenhouse Gas Emission Reductions or Removal Enhancements*. ES-UNE: Madrid, Spain, 2019.
4. *ISO 14064-2:2019; Greenhouse Gases—Part 3: Specification with Guidance for the Verification and Validation of Greenhouse Gas Statements*. ES-UNE: Madrid, Spain, 2019.
5. Cano, N.; Berrio, L.; Carvajal, E.; Arango, S. Assessing the carbon footprint of a Colombian University Campus using the UNE-ISO 14064-1 and WRI/WBCSD GHG Protocol Corporate Standard. *Environ. Sci. Pollut. Res.* **2023**, *30*, 3980–3996. [[CrossRef](#)]
6. United States Environmental Protection Agency. *Overview of Greenhouse Gases*; United States Environmental Protection Agency: Washington, DC, USA, 2014.
7. Hui, E.C.; Liang, C.; Yip, T.L. Impact of semi-obnoxious facilities and urban renewal strategy on subdivided units. *Appl. Geogr.* **2018**, *91*, 144–155. [[CrossRef](#)]
8. Cubi, E.; Doluweera, G.; Bergerson, J. Incorporation of electricity GHG emissions intensity variability into building environmental assessment. *Appl. Energy* **2015**, *159*, 62–69. [[CrossRef](#)]
9. Fang, C.L.; Wang, S.J.; Li, G.D. Changing urban forms and carbon dioxide emissions in China: A case study of 30 provincial capital cities. *Appl. Energy* **2015**, *158*, 519–531. [[CrossRef](#)]

10. Wang, S.; Fang, C.; Wang, Y.; Huang, Y.; Ma, H. Quantifying the relationship between urban development intensity and carbon dioxide emissions using a panel data analysis. *Ecol. Indic.* **2015**, *49*, 121–131. [CrossRef]
11. Ishii, S.; Tabushi, S.; Aramaki, T.; Hanaki, K. Impact of future urban form on the potential to reduce greenhouse gas emissions from residential, commercial and public buildings in Utsunomiya, Japan. *Energy Policy* **2010**, *38*, 4888–4896. [CrossRef]
12. Kim, J.; Brownstone, D. The impact of residential density on vehicle usage and fuel consumption: Evidence from national samples. *Energy Econ.* **2013**, *40*, 196–206. [CrossRef]
13. Burgalassi, D.; Luzzati, T. Urban spatial structure and environmental emissions: A survey of the literature and some empirical evidence for Italian NUTS 3 regions. *Cities* **2015**, *49*, 134–148. [CrossRef]
14. Lee, S.; Lee, B. The influence of urban form on GHG emissions in the U.S. household sector. *Energy Policy* **2014**, *68*, 534–549. [CrossRef]
15. Hachem, C. Impact of neighborhood design on energy performance and GHG emissions. *Appl. Energy* **2016**, *177*, 422–434. [CrossRef]
16. Grubler, A.; Bai, X.; Buettner, T.; Dhakal, S.; Fisk, D.; Ichinose, T.; Keirstead, J.; Sammer, G.; Satterthwaite, D.; Schulz, N.; et al. Urban energy systems. In *Glob Energy Assess—Toward a Sustainable Future*; Cambridge University Press: Cambridge, UK, 2012.
17. UNEP-DTIE Sustainable Consumption and Production Branch. In *Cities and Buildings*; UNEP: Nairobi, Kenya, 2016.
18. IEA. Buildings-Tracking Clean Energy Progress. 2019. Available online: <https://www.iea.org/tcep/buildings/> (accessed on 25 March 2019).
19. Energy Consumption Statistics Committee of China Building Energy Conservation Association. *Research Report on Building Energy Consumption in China*; Energy Consumption Statistics Committee of China Building Energy Conservation Association: Xiamen, China, 2022.
20. Roldán-Fontana, J.; Pacheco-Torres, R.; Jadraque-Gago, E.; Ordóñez, J. Optimization of CO₂ emissions in the design phases of urban planning, based on geometric characteristics: A case study of a low-density urban area in Spain. *Sustain. Sci.* **2015**, *12*, 65–85. [CrossRef]
21. Cuéllar-Franca, R.M.; Azapagic, A. Environmental impacts of the UK residential sector: Life cycle assessment of houses. *Build. Environ.* **2012**, *54*, 86–99. [CrossRef]
22. Huang, P.J.; Cui, H.; Song, J.L.; Yu, H.Y. Research on carbon emission accounting of buildings in Shanghai. *J. Shanghai Univ. Sci. Technol.* **2022**, *44*, 343–350.
23. Chen, S.; Cui, D.G.; Zhang, H.J. Building carbon emission calculation method and case study. *J. Beijing Polytech.* **2016**, *42*, 594–600.
24. Li, J.; Liu, Y. Carbon emission calculation model of construction project based on the whole life cycle. *J. Eng. Manag.* **2015**, *29*, 12–16.
25. She, J.Q.; Zhang, Y.B.; Qi, S.J. Life-cycle carbon emission characteristics and emission reduction strategies of public buildings in hot summer and warm winter zone—A case study of Xiamen City. *Build. Sci.* **2014**, *30*, 13–18.
26. Zhou, N.; McNeil, M.A.; Levine, M. *Energy for 500 Million Homes: Drivers and Outlook for Residential Energy Consumption in China*; Lawrence Berkeley National Laboratory: Berkeley, CA, USA, 2009.
27. Madlener, R.; Sunak, Y. Impacts of urbanization on urban structures and energy demand: What can we learn for urban energy planning and urbanization management? *Sustain. Cities Soc.* **2011**, *1*, 45–53. [CrossRef]
28. Chen, J.L.; Li, Z.W.; Wang, X.; Ruan, Y.J. Research on the optimization strategy of northern residential area form based on energy consumption survey. *Build. Energy Effic.* **2018**, *46*, 8–14.
29. Yang, X.; Jiang, Y. Comparison of building energy consumption between China and foreign countries. *Energy China* **2007**, *29*, 21–26.
30. Zhang, J.; Yang, Y.; Chen, X.; Mao, Q.Z. Study on the impact of residential built environment on household travel energy consumption in Jinan City. *Urban Dev. Stud.* **2013**, *20*, 83–89.
31. Liu, Z.; Chen, X.F.; Li, S.X. Ambient Microclimate: Collaborative Evaluation Process for Outdoor Thermal Comfort in the Early Design Stage. *Chin. Overseas Archit.* **2023**, 42–48.
32. Jin, H.; Cui, P. Research on the correlation between morphological elements and temperature of Harbin Central Street commercial district. *Build. Sci.* **2019**, *35*, 11–17.
33. Wei, X. Research on Reducing Carbon Consumption in Residential Community Spaces as Influenced by Microclimate Environments. *J. Urban Plan. Dev.* **2021**, *147*, 04021037. [CrossRef]
34. Yang, P.R.; Quan, J.G. Eco-volume ratio (EAR): Energy consumption assessment and carbon reduction method for urban redevelopment in high-density environment. *Urban Plan. Forum* **2014**, *3*, 61–70.
35. Zhu, R.; Wong, M.S.; You, L.; Santi, P.; Nichol, J.; Ho, H.C.; Lu, L.; Ratti, C. The effect of urban morphology on the solar capacity of threedimensional cities. *Renew. Energy* **2020**, *153*, 1111–1126. [CrossRef]
36. Zhu, R.; You, L.; Santi, P.; Wong, M.S.; Ratti, C. Solar accessibility in developing cities: A case study in Kowloon East, Hong Kong. *Sustain. Cities Soc.* **2019**, *51*, 101738. [CrossRef]
37. Vermeulen, T.; Merino, L.; Knopf-Lenoir, C.; Villon, P.; Beckers, B. Periodic urban models for optimization of passive solar irradiation. *Sol. Energy* **2018**, *162*, 67–77. [CrossRef]
38. Hachem, C.; Fazio, P.; Athienitis, A. Solar optimized residential neighborhoods: Evaluation and design methodology. *Sol. Energy* **2013**, *95*, 42–64. [CrossRef]

39. De Lemos Martins, T.A.; Adolphe, L.; Bastos, L.E.G.; de Lemos Martins, M.A. Sensitivity analysis of urban morphology factors regarding solar energy potential of buildings in a Brazilian tropical context. *Sol. Energy* **2016**, *137*, 11–24. [[CrossRef](#)]
40. Krüger, E.; Pearlmutter, D.; Rasia, F. Evaluating the impact of canyon geometry and orientation on cooling loads in a high-mass building in a hot dry environment. *Appl. Energy* **2010**, *87*, 2068–2078. [[CrossRef](#)]
41. Tsirigoti, D.; Bikas, D. A cross scale analysis of the relationship between energy efficiency and urban morphology in the Greek city context. *Procedia Environ. Sci.* **2017**, *38*, 682–687. [[CrossRef](#)]
42. Li, C.; Song, Y.; Kaza, N. Urban form and household electricity consumption: A multilevel study. *Energy Build.* **2018**, *158*, 181–193. [[CrossRef](#)]
43. Ahn, Y.J.; Sohn, D.W. The effect of neighbourhood-level urban form on residential building energy use: A GIS-based model using building energy benchmarking data in Seattle. *Energy Build.* **2019**, *196*, 124–133. [[CrossRef](#)]
44. Mouzourides, P.; Kyprianou, A.; Neophytou, M.K.A.; Ching, J.; Choudhary, R. Linking the urban-scale building energy demands with city breathability and urban form characteristics. *Sustain. Cities Soc.* **2019**, *49*, 101460. [[CrossRef](#)]
45. Swan, L.G.; Ugursal, V.I. Modeling of end-use energy consumption in the residential sector: A review of modeling techniques. *Renew. Sustain. Energy Rev.* **2009**, *13*, 1819–1835. [[CrossRef](#)]
46. Howard, B.; Parshall, L.; Thompson, J.; Hammer, S.; Dickinson, J.; Modi, V. Spatial distribution of urban building energy consumption by end use. *Energy Build.* **2012**, *45*, 141–151. [[CrossRef](#)]
47. Das, A.; Paul, S.K. CO₂ emissions from household consumption in India between 1993–94 and 2006–07: A decomposition analysis. *Energy Econ.* **2014**, *41*, 90–105. [[CrossRef](#)]
48. Robinson, D.; Campbell, N.; Gaiser, W.; Kabel, K.; Le-Mouel, A.; Morel, N.; Page, J.; Stankovic, S.; Stone, A. SUNtool—A new modelling paradigm for simulating and optimising urban sustainability. *Sol. Energy* **2007**, *81*, 1196–1211. [[CrossRef](#)]
49. Robinson, D.; Haldi, F.; Leroux, P.; Perez, D.; Rasheed, A.; Wilke, U. CitySim: Comprehensive micro-simulation of resource flows for sustainable urban planning. In Proceedings of the Eleventh International IBPSA Conference, Glasgow, UK, 27–30 July 2009; pp. 1083–1090.
50. Abbasabadi, N.; Ashayeri, M. Urban energy use modeling methods and tools: A review and an outlook. *Build. Environ.* **2019**, *161*, 106270. [[CrossRef](#)]
51. Xu, X.; Taylor, J.E.; Pisello, A.L.; Culligan, P.J. The impact of place-based affiliation networks on energy conservation: An holistic model that integrates the influence of buildings, residents and the neighborhood context. *Energy Build.* **2012**, *55*, 637–646. [[CrossRef](#)]
52. Letellier-Duchesne, S.; Nagpal, S.; Kummert, M.; Reinhart, C. Balancing demand and supply: Linking neighborhood-level building load calculations with detailed district energy network analysis models. *Energy* **2018**, *150*, 913–925. [[CrossRef](#)]
53. Pont, M.B.; Haupt, P. The relation between urban form and density M. Berghauser Pont and P. Haupt. *Urban Morphol.* **2007**, *11*, 62–65. [[CrossRef](#)]
54. Ratti, C.; Baker, N.; Steemers, K. Energy consumption and urban texture. *Energy Build.* **2005**, *37*, 762–776. [[CrossRef](#)]
55. Liu, K. *Energy Efficiency-Driven Urban form Optimization Strategy in Hot Summer and Cold Winter Areas: A Case Study of Residential Blocks in Jianhu County*; Southeast University: Nanjing, China, 2022.
56. Leng, H.; Xiao, Y.T. The influence of residential area form on residential energy consumption in cold city. *J. Harbin Inst. Technol.* **2020**, *52*, 147–156+163.
57. *JGJ26-2018; Design Standard for Energy Efficiency of Residential Buildings in Severe Cold and Cold Zones*. China Architecture & Building Press: Beijing, China, 2018.
58. *GB50736-2012; Design Code for Heating Ventilation and Air Conditioning of Civil Buildings*. China Architecture & Building Press: Beijing, China, 2012.
59. *JGJ/T449-2018; Standard for Green Performance Calculation of Civil Buildings*. China Architecture & Building Press: Beijing, China, 2018.
60. Dong, N. *Research on Low-Carbon Renewal Strategy of Old Residential Areas in Tianjin Based on Carbon Emission Accounting*; Tianjin University: Tianjin, China, 2021.
61. Privitera, R.; Palermo, V.; Martinico, F.; Fichera, A.; La Rosa, D. Towards lower carbon cities: Urban morphology contribution in climate change adaptation strategies. *Eur. Plan. Stud.* **2018**, *26*, 812–837. [[CrossRef](#)]
62. Yang, F.; Jiang, Z.D. Urban Building Cluster Energy Simulation (UBEM) and Environmentally Sustainable Oriented Urban Planning and Design: Methods, Tools and Paths. *Build. Sci.* **2019**, *37*, 17–24.
63. Leng, H.; Chen, X.; Ma, Y.H. Research progress and enlightenment of the influence of urban form on building energy consumption. *Archit. J.* **2020**, *617*, 20–126.

Disclaimer/Publisher’s Note: The statements, opinions and data contained in all publications are solely those of the individual author(s) and contributor(s) and not of MDPI and/or the editor(s). MDPI and/or the editor(s) disclaim responsibility for any injury to people or property resulting from any ideas, methods, instructions or products referred to in the content.